International Symposium
On Turbulence and Shear Flow
Phenomena (TSFP-9)
June 30 - July 3, 2015 *Melbourne, Australia*

INFLUENCE OF LARGE-SCALE MOTIONS ON EFFECTIVENESS OF ACTIVE DRAG-REDUCTION CONTROL IN TURBULENT CHANNEL FLOW AT $RE_\tau = 1000$

Bing-Qing Deng, Wei-Xi Huang, Chun-Xiao Xu and Gui-Xiang Cui
Department of Engineering Mechanics
Tsinghua University
Beijing 100084, China
xucx@tsinghua.edu.cn

ABSTRACT

Direct numerical simulations are performed in turbulent channel flows with opposition control at $Re_\tau = 180$ and 1000. The reason for the reduction of control effectiveness at higher Reynolds number is investigated. In the outer layer, the control imposed on the wall can reduce the Reynolds stresses at the same rate as the drag reduction, while the distribution of the energy at different scales is little different from the uncontrolled case. In the near-wall region at $Re_\tau = 1000$, suppression of the near-wall structures under the large-scale high-speed streaks by the control are much weaker than those under the region of the large-scale low-speed streaks, which leads to the falloff of the effectiveness of the control in suppressing the near-wall turbulence at high Reynolds numbers. By further analyzing the drag reduction rates, it is found that the effectiveness of the control is mainly determined by the suppression degree of the near-wall motions which is influenced by the large-scale motions.

INTRODUCTION

Active control of wall turbulence for skin-friction reduction is of great potential significance in industry applications. In the past two decades, quite a few active control schemes have been developed and achieved successful drag reduction in wall-bounded turbulent flows, most of which are at low Reynolds numbers ($Re_\tau \sim 10^2$). In fact, however, the practical turbulent flows posses the Reynolds numbers that usually can be higher than $Re_\tau \sim 10^5$. Therefore, whether the existing active control schemes are still effective and how the control strategies should be constructed at high Reynolds numbers must be considered.

Theoretically, the turbulent high skin friction results from the weighted integral of the Reynolds shear stress (Fukagata *et al.*, 2002). At low Reynolds numbers, the production of the Reynolds shear stress is dominated by the near-wall quasi-cyclic self-sustaining process (Panton, 2001). Therefore, interrupting any procedures of this near-wall process could possibly results in turbulence suppression and skin-friction reduction. Aiming at reducing the sweeping motion induced by the streamwise vortices, Choi *et al.* (1994) firstly proposed the so-called opposition control scheme. The direct numerical simulation (DNS) of a turbulent channel at $Re_\tau = 180$ confirmed the success of the control. The maximum drag reduction rate of 25% was obtained at $y_d^+ = 15$ accompanying with the greatly weakened streamwise vortices. Another successful example is the control by spanwise wall oscillation (Jung *et al.*, 1992). As high as 40% drag reduction was attained, and the mechanism was attributed to distorting the spatial relation between streamwise vortices and low-/high-speed streaks by the Stokes layer formed just above the oscillating surface (Choi *et al.*, 2002). However, these control schemes based on the near-wall physics become less effective in reducing the skin-friction drag at higher Reynolds numbers. In the case of opposition control, Chang *et al.* (2002) performed large-eddy simulations to turbulent channel flows at $Re_\tau = 80 - 720$ and found that the maximum drag reduction dropped from 26% at $Re_\tau = 100$ to 19% at $Re_\tau = 720$. Iwamoto *et al.* (2002) also reported that the effectiveness of the opposition control with $y_d^+ = 10$ was decreased with increasing the Reynolds number from $Re_\tau = 110 - 300$. For the control by spanwise wall oscillation, the maximum drag reduction rates also decrease as the Reynolds number increases, from 38% at $Re_\tau = 200$ to 29% at $Re_\tau = 1000$ (Touber & Leschziner, 2012). Notably, the majority of the previous studies were at the Reynolds numbers lower than $Re_\tau = 10^3$. Only very recently, the turbulent channel flows with the wall undergoing spanwise oscillating and streamwise travelling wave motions were directly simulated at $Re_\tau = 1000$ and 1600, respectively, by Agostini *et al.* (2014) and Hurst *et al.* (2014). They also reported the drag reduction decrease as the Reynolds number increase. The observed reduction in the control efficiency as the Reynolds number is increased was proposed to be related to the large-scale outer-layer structures by Touber & Leschziner (2012).

The appearance of the large-scale motions residing in and above the logarithmic region is a symbolic feature of high-Reynolds-number wall turbulence, and has drawn great attention in recent years (Marusic *et al.*, 2010*b*; Smits *et al.*, 2011). The archetypal large-scale motions are the packets of hairpin vortices that can extend several outer length scales (δ, representing channel half width, boundary layer thickness or pipe radius) in the streamwise direction and the associated low momentum region that can be longer than 10δ (large-scale low-speed streaks). The spanwise spacing of the large-scale low-speed streaks is proportional to the distance from the wall until it grows to $\lambda_z = O(\delta)$. Large-scale motions make significant contribution not only to turbulent kinetic energy but also to Reynolds shear stress and their energetic importance would further increase with

the Reynolds number (Hutchins & Marusic, 2007). Besides this, these large-scale motions also significantly affect the near-wall turbulence behaviors through superposition and modulation (Hutchins & Marusic, 2007; Mathis *et al.*, 2009; Marusic *et al.*, 2010*a*). Touber & Leschziner (2012) pointed out that an important implication of these "top-down" mechanisms is that a wall-based control strategy directed at suppressing near-wall turbulence may be less effective as the Reynolds number increases.

According to the FIK identity (Fukagata *et al.*, 2002), the contribution from Reynolds shear stress in the outer region to the skin friction would overwhelm that from the viscous inner region ($y^+ < 50$) at high Reynolds numbers. Therefore it is natural to raise the question that whether the near-wall region should still be the focus of the drag reduction control of high-Reynolds-number turbulent flows. The objective of the present work is to further clarify and quantify the contributions to the drag reduction from the inner and outer regions, why the near-wall turbulence at higher Reynolds number couldn't be damped as much as that at lower Reynolds number and what role the outer-layer large-scale structures play therein. To this end, the direct numerical simulations are performed to the opposition-controlled turbulent channel flows at $Re_\tau = 1000$ in a domain spanning $8\pi h$ and $3\pi h$ in the streamwise and spanwise directions, respectively, where h is the channel half width. The flows at $Re_\tau = 180$ in a similar large domain are also simulated for comparison.

NUMERICAL METHOD AND COMPUTATIONAL SETTING

In the present work, turbulent channel flow governed by the Navier-Stokes equations for incompressible Newtonian fluids are simulated by Fourier-Chebyshev spectral method. For the uncontrolled flows, the non-slip and impermeable conditions are used at the wall. For the controlled flows, the wall-normal velocity at the walls is specified according to the opposition control scheme (Choi *et al.*, 1994), $v_w(x,z,t) = -v(x,y_d,z,t)$. In all the simulations, the flow rates are kept constant by adjusting the driving mean pressure gradient.

In the present work, two Reynolds numbers, $Re_\tau = 180$ and 1000, are considered. The low-Reynolds-number flow is used for comparison. For $Re_\tau = 180$, the computational domain and the grid system are $8\pi \times 2 \times 4\pi$ and $288 \times 145 \times 288$, and for $Re_\tau = 1000$ they are $8\pi \times 2 \times 3\pi$ and $2304 \times 385 \times 2304$, respectively.

In the present study, the opposition control with $y_d^+ \approx 13.5$ is applied in the channel at both $Re_\tau = 180$ and 1000. The drag reduction of 23.4% and 17.8% is attained at the lower and higher Reynolds numbers, respectively. This is in agreement with the DNS results reported in literature (Choi *et al.*, 1994; Chung & Talha, 2011; Pamies *et al.*, 2007).

RESULTS AND DISCUSSION

Global Turbulence Statistics

The mean velocity profiles are shown in figure 1. The mean flows at $Re_\tau = 180$ and 1000 are both decelerated by the control in the region $y^+ < 20$, and accelerated further away from the wall, as shown in figure 1(a) because of the same flow rates for both the controlled and uncontrolled

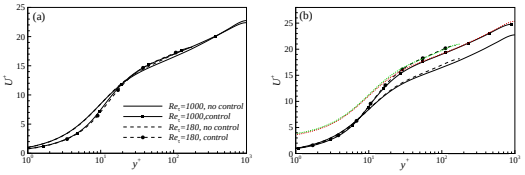

Figure 1. Mean streamwise velocity profiles normalized by (a) the uncontrolled and (b) the actual wall friction velocity. In (b), the green and red dotted lines are obtained by elevating the uncontrolled profiles at $Re_\tau = 180$ and 1000 by $\Delta U^+ = 2.8$ and 2.6, respectively.

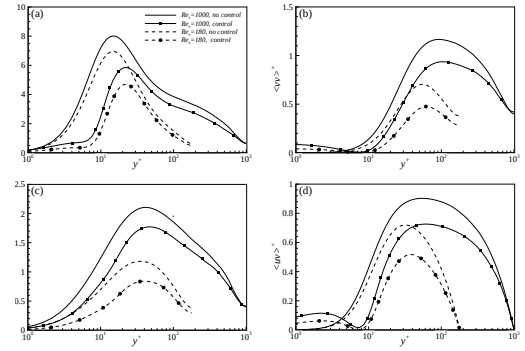

Figure 2. Reynolds stress profiles. (a) $\langle uu \rangle^+$, (b)$\langle vv \rangle^+$, (c)$\langle ww \rangle^+$ and (d)$\langle uv \rangle^+$.

flows. Scaled by the actual wall friction velocity as shown in figure 1(b), the upshifting of the logarithmic region in the controlled mean velocity profiles is more obvious at both Reynolds numbers. Elevating the uncontrolled profiles at $Re_\tau = 180$ and 1000 by $\Delta U^+ = 2.8$ and 2.6, respectively, makes them almost collapse with the controlled profiles in the outer region ($y^+ > 50$). This suggests that the absolute mean shear in the outer layer is suppressed at a degree the same as the mean wall friction τ_w. Because the drag reduction at $Re_\tau = 1000$ is lower than that at $Re_\tau = 180$, the suppression of the mean shear in the outer layer at the higher Reynolds number is also weaker than that at the lower Reynolds number.

The Reynolds stresses for both controlled and uncontrolled flows at $Re_\tau = 180$ and 1000 are shown in figure 2, which are normalized by the uncontrolled wall friction velocity at the corresponding Reynolds numbers to reveal the control effects. Near the wall, a local minimum appears in $\langle vv \rangle^+$ and $\langle uv \rangle^+$ around $y^+ = 7$ at both Reynolds numbers when the control is imposed as shown in figure 2(b) and (d), indicating the establishment of the so-called "virtual wall" between the real wall and the detection location. The turbulence fluctuations below the virtual wall are more active at $Re_\tau = 1000$ than those at $Re_\tau = 180$. Above the virtual wall, the fluctuations are globally suppressed by the control, but the suppression at higher Reynolds number is weaker than that at lower Reynolds number. For example, the near-wall peak of $\langle uu \rangle^+$ is reduced by 28% at $Re_\tau = 1000$, while at $Re_\tau = 180$ this reduction rate is 36%. The influence of the control to the inner and outer layer is also different. The suppression of all the Reynolds stress components in the outer layer is much weaker than that in the near-wall region as can be obviously seen in figure 2.

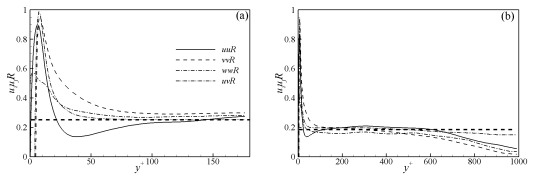

Figure 3. Reduction rate of the Reynolds stresses at (a) $Re_\tau = 180$ and (b) $Re_\tau = 1000$. The thick dashed lines indicate the corresponding mean drag reduction rates.

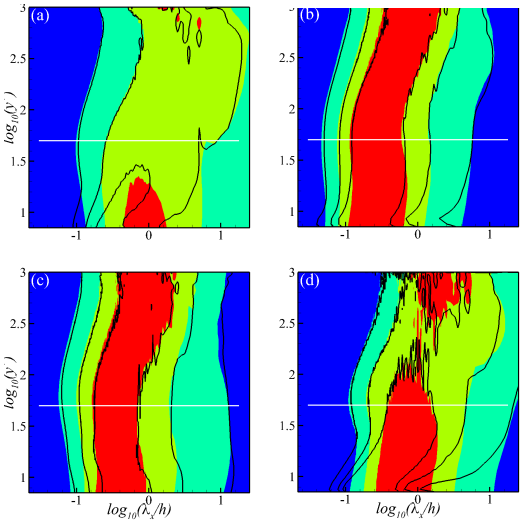

Figure 4. Pre-multiplied streamwise normalized spectra of Reynolds stresses at $Re_\tau = 1000$. (a) $k_x\phi^+_{uu}$, (b) $k_x\phi^+_{vv}$, (c) $k_x\phi^+_{ww}$ and (d) $k_x\phi^+_{uv}$. Flood: uncontrolled; Line: controlled. Contour levels: 0.05, 0.15 and 0.25. The horizontal white lines indicate $y^+ = 50$.

Motions in Outer Layer

Due to the increased contributions of the outer layer to the Reynolds stresses and hence to the control effectiveness at higher Reynolds number, the suppression of the motions, especially the large-scale motions, in the outer layer by the control will be investigated first in the following.

The influence of the control on the Reynolds stresses at different y^+ and Re_τ are quantified by the reduction rate of $\langle u_iu_j\rangle$ defined as $u_iu_jR = 1 - \langle u_iu_j\rangle^c / \langle u_iu_j\rangle^{no}$, where the superscripts "c" and "no" refer to the controlled and uncontrolled flows, respectively. As shown in figure 3, at $Re_\tau = 180$ and $Re_\tau = 1000$, the reduction rates of the Reynolds shear stress uvR in the outer layer ($y^+ > 50$) are both approximately equal to the mean drag reduction rate. At $Re_\tau = 1000$, akin to uvR, the reduction rate of the Reynolds normal stresses uuR, vvR and wwR are also close to the drag reduction rate in the region $y^+ > 100$ and $y < 0.6$. This holds from $y^+ = 100$ to the channel center at $Re_\tau = 180$.

The control effects on the partition of $\langle u_iu_j\rangle$ among different scales can be further elucidated by the spectra normalized by the corresponding Reynolds stresses, denoted as $\phi_{u_iu_j} = E_{u_iu_j}/\langle u_iu_j\rangle$. The streamwise pre-multiplied spectra of $\phi_{u_iu_j}$ above the virtual wall ($y^+ = 7$) are shown in figure 4 for both controlled and uncontrolled flows at $Re_\tau = 1000$. For the four components of the Reynolds stresses, $k_x\phi_{u_iu_j}$ in the controlled flow all collapse well with

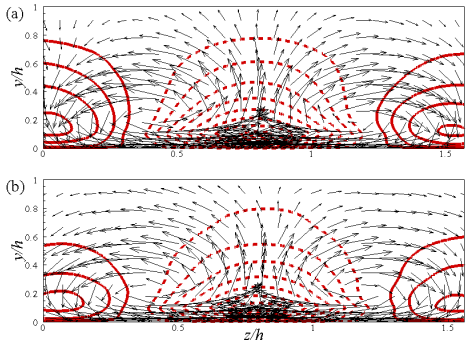

Figure 5. Conditionally averaged (v,w) vector and u contours at $Re_\tau = 1000$. (a) uncontrolled and (b) controlled. Solid and dashed lines denote positive and negative contours, respectively, with a contour level increment of 0.005.

those in the uncontrolled flow in the outer layer ($y^+ > 50$). This also stands for $k_z\phi_{u_iu_j}$. Therefore, the control does'nt change the distribution of the Reynolds stresses among different scales, and the Reynolds stresses are uniformly suppressed at different scales in the outer layer at a rate approximately equal to the drag reduction rate according to the above analysis.

Since the velocity fluctuations in the outer layer are equally suppressed at different scales by the control, the patterns of the large-scale motions wouldn't be altered. Figures 5(a) and (b) show the conditionally averaged flow field $\langle u_i(y,z) \mid u_l < 0 \text{ at } y = 0.1\rangle$ in the uncontrolled and controlled flows, where u_l is the streamwise velocity with the spanwise scale larger than h. No matter whether the control is imposed or not, the large-scale motion is a sweep-ejection pairs in the $y-z$ plane, indicating the pattern of the coherent structures are not broken by the control, but with the weakened amplitude. Additionally, in the controlled flow, these large-scale motions can still penetrate into the near-wall region.

Motions in Near-Wall Region

The influence of the large-scale motions on the near-wall region under the active control will be investigated via the analysis of the superimposition and modulation effects respectively.

Superimposition Effect Above the virtual wall there exists a kind of similarity in the controlled and uncontrolled flows. Deng *et al.* (2014) found that the controlled Reynolds shear stress could be well collapsed with the uncontrolled one by moving the coordinate origin to the virtual wall and scaling the velocity with the characteristic velocity at the virtual wall. Therefore a new coordinate y_c is defined as $y_c = y - y_{vw}$. For the uncontrolled flow $y^+_{vw} = 0$, and for the controlled flow $y^+_{vw} \approx 7$ as the detection plane is located at $y^+_d \approx 13.5$ in the present study.

Figure 6 shows the two-dimensional pre-multiplied spectra $k_xk_zE_{u_iu_j}$ at $y^+_c = 15$, the near-wall peak position of the streamwise turbulent kinetic energy, corresponding to $y^+ = 15$ and $y^+ = 22$ for the uncontrolled and the controlled flows, respectively. For the spectra of the attached variables $\langle uu\rangle$ and $\langle ww\rangle$, as shown in figure 6(a) and (c), the handles around $\lambda_x = 6h$ and $\lambda_z = h$ exist in both the uncontrolled and controlled cases, indicating that the large-scale

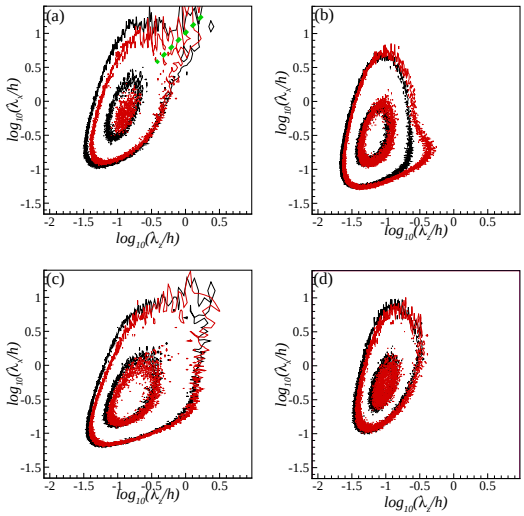

Figure 6. The two-dimensional pre-multiplied spectra of Reynolds stresses scaled by the uncontrolled friction velocity at $y_c^+ \approx 15$. (a) $k_x k_z E_{uu}$, (b) $k_x k_z E_{vv}$, (c) $k_x k_z E_{ww}$ and (d) $k_x k_z E_{-uv}$. The black and red contours refer to the uncontrolled and controlled cases at $Re_\tau = 1000$, respectively. Contour levels: (a) 0.2, 1.0; (b) 0.01, 0.05; (c)(d) 0.03, 0.15. The green dashed line in (a) is $\lambda_x = 10\lambda_z$.

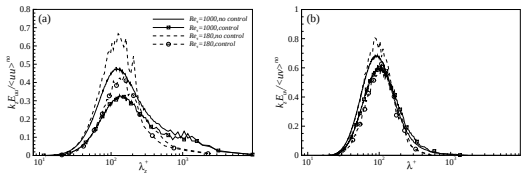

Figure 7. The pre-multiplied normalized spanwise spectra of $\langle uu \rangle$ and $\langle uv \rangle$ at $y_c^+ \approx 15$, corresponding to $y^+ \approx 15$ and 22 for the uncontrolled and controlled cases, respectively. (a) $k_z E_{uu}/\langle uu \rangle^{no}$ and (b) $k_z E_{uv}/\langle uv \rangle^{no}$.

motion can still penetrate into the near-wall region under the control. The location of the peaks in the uncontrolled flow is consistent with the typical spanwise scale of the near-wall coherent structures, i.e., $\lambda_z^+ \approx 100$. In the controlled flow, the peaks are slightly moved to the larger spanwise wavelength direction and the peak values of $k_x k_z E_{uu}$ and $k_x k_z E_{ww}$ are both suppressed. The suppression by the control is more obvious at the spanwise scales smaller than the peak-value scale. The suppression effect on the handle that represents the superimposition of the large-scale motions is weaker than that on the motions with the scales of the near-wall structures. Therefore, in the controlled flow, the contributions to $\langle uu \rangle$ and $\langle ww \rangle$ from the smaller spanwise scales are decreased, and those from the larger scales become relatively more important. For the detached variables $\langle vv \rangle$ and $\langle uv \rangle$, no contributions come from the large-scale motions ($\lambda_z > h$). The spectra shrink at the scales smaller than the characteristic scale of the near-wall structures similar to the attached variables under the control, indicating the control makes the energetic motions wider in the spanwise direction.

The above analysis shows that for the attached variables, the large-scale motions in the near-wall region is not suppressed as effectively as the near-wall structures. This may be one of the reasons why the active control becomes less effective in suppressing the near-wall attached fluctuations at higher Reynolds number. To further elucidate this issue, the spectra of the streamwise velocity at $Re_\tau = 1000$ are compared with those at $Re_\tau = 180$. Since the influence of the control on the distribution of the spectrum $k_x k_z E_{uu}$ in the spanwise direction is more conspicuous than that in the streamwise direction as shown in figure 6, the spanwise spectrum normalized by the uncontrolled streamwise kinetic energy at $y_c^+ = 15$ at $Re_\tau = 1000$ and 180 are shown in figure 7(a). In the uncontrolled flow, the spectrum at $Re_\tau = 180$ reaches a peak around $\lambda_z^+ = 125$, which corresponds to the spacing of the low-speed streaks in the near-wall region. At $Re_\tau = 1000$, the inner-peak position coincides with that at $Re_\tau = 180$, but the energy contained in the scales larger than the outer-peak scale $\lambda_z^+ = 1000$ ($\lambda_z = h$) become more significant due to the superimposition of the large-scale motions inhabiting in the logarithmic region. Therefore, around the inner peak, the ratio of the streamwise kinetic energy at $Re_\tau = 180$ is much larger than that at $Re_\tau = 1000$; while around the outer-peak scale, the ratio at the lower Reynolds number is much smaller than that at the higher Reynolds number. At $Re_\tau = 180$ the contribution from $\lambda_z^+ > 1000$ is less than 3%, but the ratio is increased to 10% at $Re_\tau = 1000$. In the controlled flow, the peaks of the spectra are moved to $\lambda_z^+ \approx 140$ by the control at both Reynolds numbers with obviously suppressed amplitudes. However, the suppression around this near-wall streak scale at $Re_\tau = 1000$ is not as strong as that at $Re_\tau = 180$. The reduction rate of the streamwise turbulent energy contained in the scales of $\lambda_z^+ < 1000$ is about 30% at $Re_\tau = 1000$, but about 35% at $Re_\tau = 180$. Therefore, one reason for the less effective suppression of the attached variables in the near-wall region at higher Reynolds number is due to the decay of the control effectiveness in the scales of the near-wall structures. On the other hand, there is about 10% of the streamwise kinetic energy contained in the scales of $\lambda_z^+ > 1000$ at $Re_\tau = 1000$, but the suppression of the large-scale motion is far less than that at the small scales around the inner peak. The weaker suppression of the large-scale motions than the near-wall structures further deteriorates the suppression of $\langle uu \rangle$ at higher Reynolds number.

The decay of the control effectiveness in suppressing the near-wall structures can also be found in the detached variables, such as the Reynolds shear stress $\langle uv \rangle$, in which there is almost no contributions from the scales of $\lambda_z > h$ ($\lambda_z^+ > 1000$) in the near-wall region. The spanwise spectrum of $\langle uv \rangle$ at $y_c^+ = 15$ is shown in figure 7(b). As expected, the pre-multiplied spectrum $k_z E_{uv}$ tends to zero at $\lambda_z^+ > 1000$. Therefore, the control effect of the detached variables is determined by the near-wall structures. The peak of the spectrum is shifted from $\lambda_z^+ \approx 91$ to $\lambda_z^+ \approx 110$ by the control at these two Reynolds numbers. Consistent with the spectrum shown in figure 6(d), the suppression of the Reynolds shear stress is mainly at the scales smaller than the peak-value scale, and the suppression at the lower Reynolds number is much stronger than that at the higher Reynolds number.

Modulation effect In the near-wall region, the small-scale motions tend to be modulated by the large scales (Hutchins & Marusic, 2007). Mathis *et al.* (2009) found that near the wall the small-scale fluctuations are more intensi-

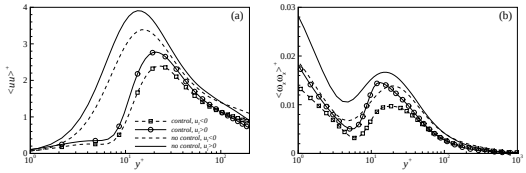

Figure 8. Intensity of the streamwise fluctuating velocity and vorticity in the region of $u_l < 0$ and $u_l > 0$ at $Re_\tau = 1000$.

fied in the large-scale high-speed regions than in the low-speed regions. In the present work, the velocity fluctuation is decomposed into large and small-scale components using a spectral filter to study the modulation effect. The large-scale component is obtained by low-pass filtering the signal in the spanwise direction and denoted by the subscript "l". The filter width is chosen to be $\lambda_z = h$ ($\lambda_z^+ = 1000$).

Figure 8(a) shows the streamwise kinetic energy conditionally averaged in the large-scale high-speed ($u_l > 0$) and low-speed ($u_l < 0$) regions, respectively. Consistent with Hutchins & Marusic (2007) and Mathis *et al.* (2009), in the uncontrolled flow, the streamwise velocity fluctuation in regions of $u_l > 0$ is much stronger than that in regions of $u_l < 0$. The peak location with $u_l > 0$ is around $y^+ = 13.5$, while that with $u_l < 0$ locates further away from the wall at $y^+ \approx 15.5$. When the control applies, $\langle uu \rangle^+$ is globally suppressed but the modulation effect still exists, as indicated by the different peak values in $u_l > 0$ and $u_l < 0$ regions. The peaks of $\langle uu \rangle^+$ are pushed about 7 wall units away from the wall by the control, a distance between the virtual wall and the real wall, in both positive and negative u_l regions of the controlled flow.

Not only the amplitude and the location of the small-scale streaks are modulated by the large-scale motion, the near-wall streamwise vortices are also significantly influenced. As shown in figure 8(b), in the uncontrolled flows, the amplitude of $\langle \omega_x \omega_x \rangle^+$ with $u_l > 0$ is obviously larger than that with $u_l < 0$ in the near-wall region. The location of the interior peak with $u_l > 0$ is around $y^+ = 16$, while that with $u_l < 0$ is at $y^+ \approx 20$. The local minimum positions in both cases are almost the same. These observations indicate that statistically the streamwise vortices in the large-scale high-speed regions are stronger and smaller with the core closer to the wall than those in the large-scale low-speed regions. In the controlled flows, the amplitudes of $\langle \omega_x \omega_x \rangle^+$ are both attenuated in $u_l > 0$ and $u_l < 0$ regions. Although the local minimum positions are pushed a little bit away from the wall in both cases, the interior maximum positions are drawn closer to the wall by the control. The interior peak with $u_l > 0$ is moved from $y^+ \approx 16$ to $y^+ \approx 13.5$ by the control, and that with $u_l < 0$ is changed from $y^+ \approx 20$ to $y^+ \approx 18.5$. This indicates that the averaged radius of the streamwise vortices become smaller in both $u_l > 0$ and $u_l < 0$ regions under the control. The modulation effects are obviously exhibited in the amplitude of $\langle \omega_x \omega_x \rangle^+$ under the control. The suppression of $\langle \omega_x \omega_x \rangle^+$ in the region of $u_l > 0$ is significantly weaker than that in the region of $u_l < 0$. The reduction rate of the peak value of $\langle \omega_x \omega_x \rangle$ with $u_l > 0$ is about 14%, while that with $u_l < 0$ is around 30%. As a reference, the reduction rate of the peak value of the total $\langle \omega_x \omega_x \rangle$ is around 40% at $Re_\tau = 180$.

Since the streamwise vortices are closely related to the generation of Reynolds shear stress in the near-wall region, the weakened effect in attenuating the streamwise vortices in the region $u_l > 0$ implies that the Reynolds shear stress in this region is not effectively suppressed. The conditional statistics shows that the reduction rate of the Reynolds shear stress in the region $u_l > 0$ is much smaller than that in the region $u_l < 0$, indicating the less effectiveness of the control in suppressing the near-wall structures is closely related to the modulation effect of the large-scale motions, especially the high-speed large-scale motion.

Contribution to Drag Reduction Rate From Inner and Outer Regions

In turbulent channel flow, the mean wall shear stress can be expressed as (Fukagata *et al.*, 2002):

$$\tau_w = \frac{3\mu U_m}{h} + 3\rho \int_0^1 (1-y)\langle -uv \rangle \mathrm{d}y, \qquad (1)$$

which stands for both uncontrolled and controlled flows. In case of the fixed flow rate, the mean drag reduction rate, which can be written into $DR = (\tau_w^{no} - \tau_w^c)/\rho(u_\tau^{no})^2$, can be obtained according to equation (1):

$$DR = 3\int_0^1 (1-y)(\langle -uv \rangle^{no+} - \langle -uv \rangle^{c+})\mathrm{d}y, \qquad (2)$$

in which the superscript "$^+$" indicates the normalization by u_τ^{no}. Denote the integral of the Reynolds shear stress as $I = \int_0^1 (1-y)\langle -uv \rangle^+ \mathrm{d}y$, and that in the outer and inner regions as $I_{outer} = \int_{y_t}^1 (1-y)\langle -uv \rangle^+ \mathrm{d}y$, and $I_{inner} = \int_0^{y_t} (1-y)\langle -uv \rangle^+ \mathrm{d}y$, respectively. Equation (2) can be represented by

$$DR = 3(I_{inner}^{no} - I_{inner}^c) + 3(I_{outer}^{no} - I_{outer}^c) \qquad (3)$$

According to figure 3, the reduction rate of the Reynolds shear stress in the region of $y^+ > 50$ is almost equal to the mean drag reduction rate. Therefore, if choosing $y_t^+ = 50$, we can have $I_{outer}^c = (1-DR)I_{outer}^{no}$. Let IR_{inner} denotes the reduction rate of the integral of the Reynolds shear stress in the inner region, i.e., $IR_{inner} = 1 - I_{inner}^c / I_{inner}^{no}$, the drag reduction rate can be further written into

$$DR = IR_{inner} \frac{3I_{inner}^{no}}{1 - 3I_{outer}^{no}} = IR_{inner} IR_{in/out}, \qquad (4)$$

where $IR_{in/out} = 3I_{inner}/(1 - 3I_{outer})$ embodies the influence of the Reynolds shear stress in the outer layer. The values of $IR_{in/out}$ at different Reynolds numbers are computed using the present uncontrolled data at $Re_\tau = 180$ and 1000 and the data of Hoyas & Jiménez (2006) at $Re_\tau = 550$ and 2000. It is found that $IR_{in/out}$ increases with the Reynolds number, for example, $IR_{in/out} = 0.58$, 0.62, 0.66 and 0.78 at $Re_\tau = 180$, 550, 1000, and 2000, respectively. Considering the drag reduction of 17.8% at $Re_\tau = 1000$ in comparison with that of 23.4% at $Re_\tau = 180$, it can be concluded that the reason for the decayed drag reduction rate at higher Reynolds numbers is attributed to the lessened effectiveness of the control in suppressing the near-wall coherent structures.

Summary

In the present study, direct numerical simulations are performed to turbulent channel flows at $Re_\tau = 1000$ with wall blowing and suction determined by the opposition control scheme. The flows at $Re_\tau = 180$ are also simulated for comparison. As the Reynolds number increases, the drag reduction by the control drops from 23.4% to 17.8%.

Under the normalization by their actual wall friction velocity, the controlled and uncontrolled mean velocity profiles collapse together in the outer layer by elevating the uncontrolled one a constant ΔU^+, indicating that the control reduces the mean shear in the outer layer at a rate the same as the mean wall friction. The reduction of the Reynolds shear stress is also identical to the mean drag reduction rate in $y^+ > 50$. These results hold for both higher and lower Reynolds numbers. Furthermore, it is shown at $Re_\tau = 1000$ that the Reynolds stresses are equally suppressed by the control at different scales, and the large-scale motions keep the same pattern but with a reduced intensity under the manipulation of the control.

The effects of the control on the motions near the wall weakens as the Reynolds number increases. The role the large-scale motions play therein is investigated from the viewpoint of "top-down" influence mechanism. At $Re_\tau = 1000$, the large-scale contribution via superimposition to the near-wall streamwise kinetic energy becomes larger compared with that at $Re_\tau = 180$, but the suppression by the control at large scales is weaker than that at small scales. Furthermore, the small-scale Reynolds stresses are also less reduced at higher Reynolds number than at lower Reynolds number. The streamwise kinetic energy and enstrophy in the large-scale high-speed regions are less effectively affected by the control than those in the low-speed regions. Correspondingly the contribution to the reduction of the Reynolds shear stress from large-scale high-speed regions is lower than that from the low-speed regions.

To quantify the respective contributions to drag reduction from inner and outer layers, theoretical analysis is performed based on the FIK identity. Considering that the reduction rate of the Reynolds shear stress in $y^+ > 50$ approximately equals to the mean drag reduction rate, a formula is derived out and describes the direct relation between the reduction rates of the mean friction drag and the integral of the inner-layer weighted Reynolds shear stress. It is demonstrated that the drop in the drag reduction rate at high Reynolds number is due to the inefficient manipulation of the near-wall motions, which is exposed to the "top-down" influence of the large-scale motions in the high Reynolds number case. Therefore how to effectively manipulate the near-wall structures under the influence of the large-scale motions embedded in the outer layer is a crucial issue for drag reduction control in high-Reynolds-number wall-bounded turbulent flows.

Acknowledgments The work is supported by National Natural Science Foundation of China (Project No. 11490551, 11472154, 11322221, 11132005).

REFERENCES

Agostini, L., Touber, E. & Leschziner, A. 2014 Spanwise oscillatory wall motion in channel flow: drag-reduction mechanisms inferred from DNS-predicted phase-wise property variations at $Re_\tau = 1000$. *J. Fluid Mech.* **743**, 606–635.

Chang, Y., Collis, S. S. & Ramakrishnan, S. 2002 Viscous effect in control of near-wall turbulence. *Phys. Fluids* **14**, 4069–4080.

Choi, H., Moin, P. & Kim, J. 1994 Active turbulence control for drag reduction in wall-bounded flows. *J. Fluid Mech.* **262**, 75–110.

Choi, J. I., Xu, C. X. & Sung, H. J. 2002 Drag reduction by spanwise wall oscillation in wall-bounded turbulent flows. *AIAA J.* **40**, 842–850.

Chung, Y. M. & Talha, T. 2011 Effectiveness of active flow control for turbulent skin friction drag reduction. *Phys. Fluids* **23**, 025102.

Deng, B. Q., Xu, C. X., Huang, W. X. & Cui, G. X. 2014 Strengthened opposition control for skin-friction reduction in wall-bounded turbulent flows. *J. Turb.* **15(2)**, 122–143.

Fukagata, K., Iwamoto, K. & Kasagi, N. 2002 Contribution of Reynolds stress distribution to the skin friction in wall-bounded flow. *Phys.Fluids* **14**, L73.

Ganapathisubramani, B., Hutchins, N., Monty, J. P., Chung, D. & Marusic, I. 2012 Amplitude and frequency modulation in wall turbulence. *J. FLuid Mech.* **712**, 61–91.

Hoyas, S. & Jiménez, J. 2006 Scaling of the velocity fluctuations in turbulent channels up to $Re_\tau = 2003$. *Phys. Fluids* **18**, 011702.

Hurst, E., Yang, Q. & Chung, Y. M. 2014 Effect of Reynolds number on turbulent drag reduction by streamwise travelling waves. *J. Fluid Mecha.* **759**, 28–55.

Hutchins, N. & Marusic, I. 2007 Large-scale influence in near-wall turbulence. *Phil. Trans. R. Soc. Lond. A* **365**, 647–664.

Iwamoto, K., Suzuki, Y. & Kasagi, N. 2002 Reynolds number effect on wall turbulence: toward effective feedback control. *Int. J. Heat Fluid Flow* **23**, 678–689.

Jung, W. J., Mangiavacchi, N. & Akhavan, R. 1992 Suppression of turbulence in wall-bounded flows by high-frequency spanwise oscillation. *Phys. Fluids A* **4**, 1605–1607.

Marusic, I., Mathis, R. & Hutchins, N. 2010*a* Predictive model for wall-bounded turbulent flows. *Science* **329**, 193–196.

Marusic, I., McKeon, B. J., Monkewitz, P. A., Nagib, H. M. & Smits, A. J. 2010*b* Wall-bounded turbulent flows at high Reynolds numbers: Recent advances and key issues. *Phys. Fluids* **22**, 065103.

Mathis, R., Hutchins, N. & Marusic, I. 2009 Large-scale amplitude modulation of the small-scale structures of turbulent boundary layers. *J. Fluid Mech.* **628**, 311–337.

Pamies, M., Garnier, E., Merlen, A. & Sagaut, P. 2007 Response of a spatially developing turbulent boundary layer to active control strategies in the framework of opposition control. *Phys.Fluids* **19**, 108102.

Panton, R. L. 2001 Overview of the self-sustaining mechanisms of wall turbulence. *Prog. Aero. Sci.* **37**, 341–383.

Smits, A. J., Mckeon, B. J. & Marusic, I. 2011 High Reynolds number wall turbulence. *Annu. Rev. Fluids Mech.* **43**, 353–375.

Touber, E. & Leschziner, M. A. 2012 Near-wall streak modification by spanwise oscillatory wall motion and drag reduction mechanisms. *J. Fluid Mech.* **693**, 150–200.